



# Flood Susceptibility Assessment in Bangladesh Using Machine Learning and Multi-criteria Decision Analysis

Mahfuzur Rahman<sup>1,2,3</sup> · Chen Ningsheng<sup>1</sup> · Md Monirul Islam<sup>3</sup> · Ashraf Dewan<sup>4</sup> · Javed Iqbal<sup>1,5</sup> · Rana Muhammad Ali Washakh<sup>1,2</sup> · Tian Shufeng<sup>1,2</sup>

Received: 29 July 2019 / Accepted: 21 September 2019 / Published online: 14 October 2019  
© King Abdulaziz University and Springer Nature Switzerland AG 2019

## Abstract

This work proposes a new approach by integrating statistical, machine learning, and multi-criteria decision analysis, including artificial neural network (ANN), logistic regression (LR), frequency ratio (FR), and analytical hierarchy process (AHP). Dependent (flood inventory) and independent variables (flood causative factors) were prepared using remote sensing data and the Mike-11 hydrological model and secondary data from different sources. The flood inventory map was randomly divided into training and testing datasets, where 334 flood locations (70%) were used for training and the remaining 141 locations (30%) were employed for testing. Using the area under the receiver operating curve (AUROC), predictive power of the model was tested. The results revealed that LR model had the highest success rate (81.60%) and prediction rate (86.80%), among others. Furthermore, different combinations of the models were evaluated for flood susceptibility mapping and the best combination ( $I_1C$ ) was used for generating a new flood hazard map for Bangladesh. The performance of the  $I_1C$  integrated models was also evaluated using the AUROC and found that integrated LR-FR model had the highest predictive power with an AUROC value of 88.10%. This study offers a new opportunity to the relevant authority for planning and designing flood control measures.

**Keywords** AHP · ANN · Bangladesh · Flood susceptibility map · FR · LR

## 1 Introduction

Bangladesh is one of the most disaster-prone countries in the world. Flat topography, shallow riverbed, severe monsoonal rainfall, and huge discharge of sediments are major factors responsible for floods in Bangladesh (Hossain 2015;

Rahman et al. 2007; Sinha 2007). Therefore, identifying areas prone to floods is very important to reduce the loss of lives and properties. The flood event of 2017 (including floods in 1954, 1955, 1974, 1987, 1988, 1995, 1998, 2004, 2007, and 2014) caused enormous damage to property and considerable loss of lives. The heavy rainfall from

✉ Chen Ningsheng  
chennsh@imde.ac.cn

Mahfuzur Rahman  
mfz.rahman@iubat.edu

Md Monirul Islam  
mmislam@iubat.edu

Ashraf Dewan  
a.dewan@curtin.edu.au

Javed Iqbal  
javediqbalgeo@gmail.com

Rana Muhammad Ali Washakh  
washakh@qq.com

Tian Shufeng  
tiansf@imde.ac.cn

<sup>1</sup> Key Laboratory for Mountain Hazards and Earth Surface Process, Institute of Mountain Hazards and Environment, Chinese Academy of Sciences (CAS), Chengdu 610041, People's Republic of China

<sup>2</sup> University of Chinese Academy of Sciences, Beijing 100049, People's Republic of China

<sup>3</sup> Department of Civil Engineering, International University of Business Agriculture and Technology (IUBAT), Dhaka, Bangladesh

<sup>4</sup> Spatial Sciences Discipline, School of Earth and Planetary Sciences, Curtin University, Kent St, Bentley, WA 6102, Australia

<sup>5</sup> Department of Earth Sciences, Abbottabad University of Science and Technology, Abbottabad, Pakistan

upper-basin (upper and lower Brahmaputra, Kyaichinang, Barak, and so on) and lower-basin (the Ganges–Brahmaputra–Meghna basin) was accountable for severe flooding in Bangladesh in 2017. Because it turns into runoffs, due to the rough terrain and the vegetation situation in the area and such runoffs soon flow as floodwater. More than 30% areas were affected by the flood in 2017 (Uddin et al. 2019). It disrupted daily life, causing at least 134 deaths and nearly affected six million people across the country (Uddin et al. 2019). Cumulative discharge in the Brahmaputra and the Jamuna rivers within the country was increasing due to excessive rainfall in China, Nepal, and India, and as a result, water could not be drained out properly into the Bay of Bengal as reported by Bangladesh Water Development Board (BWDB).

Flood susceptibility mapping can be defined as a quantitative or qualitative assessment of the classification, area, and spatial distribution of flood, which exists or potentially may occur in an area. Therefore, flood susceptibility mapping can help policymakers and relevant authorities to create emergency plans. It was stated that the occurrence of flood hazards cannot be stopped, but damages from flood could be avoided or substantially reduced if flood-affected areas were identified accurately (Sahoo and Sreeja 2015). Therefore, flood susceptibility assessment is very crucial for disasters alleviation. A broad range of model has been suggested by researchers to assess flood hazards. Most of the recent models were mainly focused on hydrological models, hydrodynamic models, multi-criteria decision analysis (MCDA), statistical models (SM), and machine learning (ML) techniques incorporated into geographical information system (GIS) (Danumah et al. 2016; de Brito and Evers 2016; Elsafi 2014; Fernández and Lutz 2010; Lee et al. 2012; Luu et al. 2018; Rahmati et al. 2016c; Rao 2017; Shafapour Tehrany et al. 2017; Tehrany et al. 2014a; Yang et al. 2014). GIS and remote sensing are also important tools, which have been used extensively for hazard assessment (Ashley et al. 2014; Barua et al. 2016; Fernández and Lutz 2010; Islam and Sado 2000a; Kia et al. 2012; Luu et al. 2018; Shafapour Tehrany et al. 2017; Tehrany et al. 2014b). Studies have revealed that MCDA models are better for flood assessment. AHP is a popular model in the field of MCDA, because it can solve complex decision problem without any data (Danumah et al. 2016; Fernández and Lutz 2010; Luu et al. 2018). Besides, the most popular machine learning and statistical models in natural hazards analysis are artificial neural networks (ANN) (Elsafi 2014; Kia et al. 2012), logistic regression (LR) (Arabameri et al. 2018; Hong et al. 2015; Shafapour Tehrany et al. 2017; Tehrany et al. 2014a), frequency ratio (FR) (Pradhan and Lee 2010; Samanta et al. 2018b; Tehrany et al. 2019), weight-of-evidence (WoE) (Shafapour Tehrany et al. 2017; Tehrany et al. 2014b), and support vector machine (SVM) (Chen et al. 2018; Hong et al. 2015; Tehrany et al.

2015b). These models have perfect and consistent prediction capability for flood hazard occurrences (Bui et al. 2018; Chapi et al. 2017; Tehrany et al. 2014a), while hydrological and hydrodynamic models have some limitations, including time-consuming, requires careful and accurate calibration to yield accurate estimates of flood affected areas (Asare-Kyei et al. 2015; Fencia et al. 2014).

Although many researchers have conducted flood studies in various locations worldwide (Chapi et al. 2017; Dewan et al. 2007; Khosravi et al. 2016a; Masood and Takeuchi 2012; Seejata et al. 2018; Tingsanchali and Karim 2005), to the best of our knowledge, none of them integrated ML, SM models, and MCDA models for the development of flood susceptibility mapping, particularly for Bangladesh. Moreover, the traditional method for flood susceptibility mapping in Bangladesh is the hydrological and hydrodynamic models, which require input data and parameters from meteorology, river cross-sections, and discharge from both upstream and downstream (Khosravi et al. 2016b, 2018). These data are mostly unavailable for many areas, due to inadequate hydro-meteorological stations. At present, flood inundation area map is produced by the Flood Forecasting and Warning Centre (FFWC) by comparing river water level with a coarse resolution (cf. 500 m) digital elevation model (DEM). Unfortunately, a high-resolution DEM and infrastructures data are not available (Bates 2004). Flood susceptibility assessment based on water level observation is not effective in providing spatially distributed flooding areas for timely monitoring of flooding event (Lin et al. 2019; Uddin et al. 2019). Therefore, the techniques used in the present study proved to be the best opportunity for relatively large and complex areas.

The main objective of this research is to derive the extent of flood susceptibility areas in Bangladesh using four models: artificial neural network (ANN), analytical hierarchy process (AHP), logistic regression (LR), and frequency ratio (FR). The flood hazard map for Bangladesh was developed previously by considering flood frequency, flood duration with digital elevation data (Islam and Sado 2000b, 2002; Masood and Takeuchi 2012; Tingsanchali and Karim 2005), while in this study we have proposed nine causative factors for flooding, i.e. rainfall, elevation, slope, flood depth, soil tract, geology, drainage area, flood duration, and land cover and land use (LULC). Besides, applying only one model will not be adequate to predict the susceptible areas in a study. Because, these models are mostly site specific and some research has confirmed that each model has its advantages and disadvantages. Therefore, the second objective is to derive an integrated model, considering the best performing models, to develop a unique flood hazard map of Bangladesh, because model integration is expected to allow more precise assessment (Chapi et al. 2017; Costache and Zaharia 2017; Khosravi et al. 2016a; Mojaddadi et al. 2017;

Shafapour Tehrani et al. 2017). The key contributions of this research are: (i) to generate relevant models for the determination of flood susceptible areas; and (ii) produce new flood hazard map for Bangladesh, using an integrated model.

## 2 Materials and Methods

### 2.1 Study Area

The climatic condition makes Bangladesh the most vulnerable country in the world to multiple hazards. This is a nation of over 162.7 million people (Bangladesh Bureau of Statistics B 2019) with a geographical area of 1, 47,570 sq. km located between 20°34'N and 88°01'E to 26°38'N and 92°41'E (Hasan et al. 2017). An annual growth rate of the population of Bangladesh is 1.37%, and therefore, is one of the most densely populated countries in the world having a population density of 1062.5 per sq.km (Hasan et al. 2017). A location map of Bangladesh is shown in Fig. 1. The country has 492 sub-districts and it is divided into five main physiographic regions, namely north Bengal region, northeastern region, Tippera-Comilla region, southwestern region, and Chittagong region, with various subdivisions (Islam and Sado 2000b). It is crisscrossed by three mighty rivers: the Ganges, Brahmaputra, and Meghna, popularly known as GBM. The alluvial soil deposited by these rivers

has created highly fertile lands. It has three distinctive features: (i) a broad alluvial plain subject to frequent flooding, (ii) a slightly elevated relatively older plain, and (iii) a small hilly region drained by flashy rivers. The alluvial plain is a part of the larger plain of the Bengal, which is sometimes called the Lower Gangetic Plain. Elevations of the plains are less than 10 m above sea level. The hilly areas of the southeastern region of Chittagong, the northeastern hills of Sylhet and highlands in the north and northwest are of low height. The Chittagong Hills constitute the only significant hilly system in the country. The climate of the country is tropical and humid. The annual average rainfall varies between 2200 mm and 2500 mm, whereas extreme rainfall varies from 1200 mm to 6500 mm. The average temperature varies from 25 to 35 °C, during a year.

### 2.2 Data Preparation

Rainfall data were collected from Bangladesh Water Development Board (BWDB) and NOAA satellite images generated by NASA's global precipitation measurement (GPM) mission. The digital elevation model (DEM) data with a spatial resolution of 300 m were obtained from Institute of Water Modeling (IWM) (Islam and Sado 2000b). The slope layer was extracted from DEM. A LULC map was obtained from the existing map produced by Space Research and Remote Sensing Organization (SPARRSO) (Islam and Sado 2000a) and updated by the Forest Department of Bangladesh in 2016 (Department 2016). The geological map of Bangladesh was obtained from Geological Survey of Bangladesh. The soil tract map with 1:100,000 scale for the study area was acquired from the Bangladesh Agricultural Research Council (BARC) and Soil Resource Development Institute (SRDI). The drainage areas' data were collected from Bangladesh Agricultural Research Council (BARC). The flood depth in the study area was calculated by subtracting the land elevation from the computed flood water level (Tingsanchali and Karim 2005). The flood duration was determined using satellite images having spatial resolution of 12.5 m developed by International Centre for Integrated Mountain Development (ICIMOD) from Advanced Land Observing Satellite-2 (ALOS-2), Phased Array L-band Synthetic Aperture Radar (PALSAR) and Sentinel-1) of June 24, July 17, August 15, and August 24 of 2017. The 2017 flood inundated most of the floodplain areas and lasted for more than 24 days according to field investigation done by flood forecasting department and observed hydrological data.

### 2.3 Computing Flood Inundation Area

Flood inundation areas were calculated through remote sensing data analysis, Mike-11 hydrological model outputs, and three severe historical flood events of 1988, 1995, and 1998.

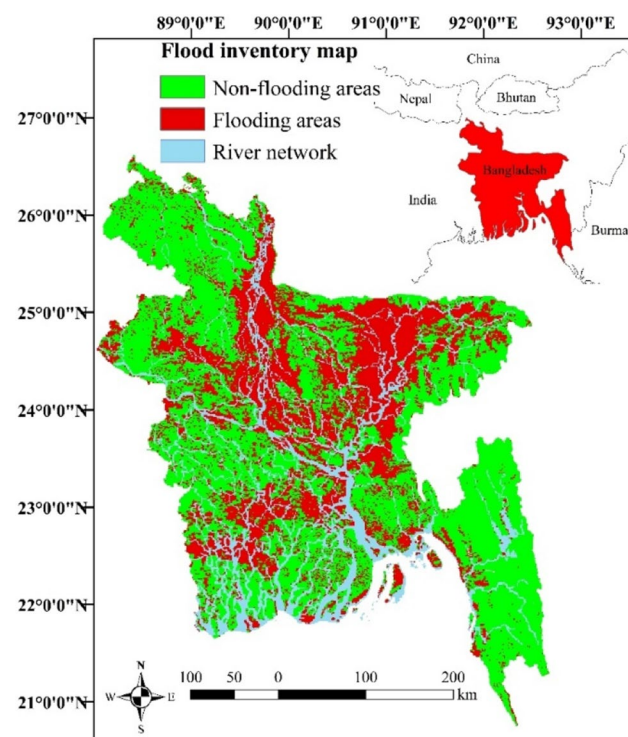


Fig. 1 Location of the study area

The details of calculations are as follows: (i) first, we considered four flood inundation maps of June 24, 2017, July 17, 2017, August 15, 2017, and August 24, 2017, which were prepared by ICIMOD considering the remote sensing imageries from ALOS-2, PALSAR, and Sentinel-1 imagery (ICIMOD 2017). The images were transformed into coordinate system (WGS 1984/UTM45N) based on an administrative map of Bangladesh. (ii) Second, Mike-11 hydrodynamic model output maps of Bangladesh Water Development Board were used to calculate flood inundation area considering the same dates of June 24, 2017, July 17, 2017, August 15, 2017, and August 24, 2017. The Mike-11 model solves the unsteady free surface flow equations of continuity and momentum (Tingsanchali and Karim 2005). The DEM having 300 m spatial resolution was used with Mike-11. Finally, remote sensing imageries and Mike-11 model output maps were compared to estimate flood inundation areas. To create the final flood inventory map, National Oceanic and Atmospheric Administration (NOAA) advanced very high-resolution radiometer (AVHRR) data for the flood events of 1988, 1995, and 1998 were incorporated with flood inundation areas (the inundated areas that did not appear in any of the images mentioned in this study were considered to be non-flooding areas, while the inundated areas appeared in all images were considered to be flooding areas), which were used to analyze the correlation between flood and flood conditioning factors. A flood inventory is a detailed register of the distribution and characteristics of past flood events. In the present study, the presence of flood was consigned a value of 1, while the absence of flood was consigned a value of 0 for preparing flood inventory map from flood inundation areas (Bui et al. 2018; Darabi et al. 2019). Finally, the values of all the flood conditioning factors were extracted to flooding and non-flooding points to form training and validation datasets. We identified 475 flood locations from where 70% of the locations were randomly selected for training and the rest were considered for validation.

## 2.4 Factors Affecting Flood Susceptibility

To prepare flood susceptibility maps, various thematic layers were used as conditioning factors. Rainfall is the main triggering factor that causes underground hydrostatic level and water pressure to increase. Mostly, heavy rainfall from upstream point (India) is the major reason for occurrence of flood in Bangladesh. The recorded rainfall amount during the monsoon period of 2017 varies from 120.10 mm to 898.62 mm (BWDB 2017). Land elevation is another factor in the assessment of flood susceptibility (Rizeei et al. 2019). Runoff flows from high to low lands, therefore the probability of flood occurrence in low-elevated areas increases. Sometimes, lowland areas did not flood, while some high land elevation areas were flooded, due to

flash floods in the northeastern part of the country. The elevation of the study area ranges from 0 to above 80 m of mean sea level. The likelihood of a flood increases, as the slope of a location decreases, making it a reliable indicator for flood susceptibility. Therefore, slope plays a major role in flooding and it also affects the direction of water flow. Land use and land cover map is one of the most important factors affecting floods, because vegetated areas are less susceptible for flooding due to the negative correlation between a flooding event and vegetation density (Mojaddadi et al. 2017). However, urban areas are typically composed of impermeable surfaces and increased surface runoff, therefore it can be concluded that runoff conditions vary under different LULC patterns. Besides, LULC has a direct impact on a number of parameters in the hydrologic cycle, including interception, infiltration, and concentration, and therefore indirectly on flooding. Together, these characteristics yield information about the hydrological response and the degree of flood hazard (Islam and Sado 2000b). The geological factor of the study area is covered with various types of units, which directly or indirectly influence infiltration and runoff generation, depending on the porosity and permeability of soil and rock (Rahmati et al. 2016b). Moreover, geology significantly affects the formation of the drainage pattern that relates to the generation of floodplain (Bui et al. 2019). Islam and Sado (2000a) reported that largely impermeable surface geology areas are more susceptible to flooding. Therefore, geological units play an important role. The water infiltration initially depends upon soil properties (Rahmati et al. 2016b); therefore, soil group is another important conditioning factor. Todini et al. (2004) and Nyarko (2002) mentioned that the soil type plays a role in determining the water holding characteristics of an area, and hence affects flood susceptibility. Moreover, flood depth and flood duration directly contribute to flood occurrence. The classification methods of flood conditioning factors are shown in Table 1 and thematic maps for flood conditioning factors are shown in Fig. 2.

Furthermore, multicollinearity among all the factors was checked using the tolerance (TOL) and variance inflation factor (VIF), since linear collinearity between the conditioning factors will decrease the model prediction accuracy (Rahmati et al. 2016a). The coefficient values of TOL and VIF were below 0.10 and above 10.0, respectively, indicating the existence of collinearity between conditioning factors (Arabameri et al. 2019; Chen et al. 2018). The coefficient values for  $TOL < 0.10$  and  $VIF > 10$  indicated high multicollinearity between factors being considered. The results of the multicollinearity showed that no multicollinearity was present, among the nine factors used (Table 2).

**Table 1** Flood conditioning factors and classification scheme for flood susceptibility assessment

Flood conditioning factors	Classes	Method and reference
Rainfall (mm)	(i) Above 600; (ii) 401 to 600; (iii) 201 to 400; and (iv) 0 to 200.	Equal interval [(Pham et al. 2017)]
Elevation (m)	(i) 0 to 4; (ii) 4 to 8; (iii) 8 to 12; (iv) 12 to 16; (v) 16 to 20; (vi) 20 to 40; (vii) 40 to 60; (viii) 60 to 80; and (ix) above 80.	Manual [(Islam and Sado 2000a)]
Slope (°)	(i) 0° to 10°; (ii) 10° to 20°; (iii) 20° to 30°; (iv) 30° to 40°; (v) 40° to 50°; (vi) 50° to 60°; (vii) 60° to 70°; and (viii) 70° to 80°.	Equal interval [(Ouma and Tateishi 2014; Rahmati et al. 2016c; Seejata et al. 2018)]
LULC	(i) Cultivated land; (ii) boro rice field; (iii) cultivated lowland; (iv) dry fallows; (v) mixed cropped areas; (vi) mangrove area; (vii) highland with mixed forest; (viii) highland with settlements; (ix) saline area; and (x) watercourse/river.	Supervised classification [(Islam and Sado 2000a)]
Geology	(i) Coastal deposits: beach and dune sand; (ii) deltaic deposits: silt, sand, tidal mud, and so on; (iii) alluvial deposits: alluvial sand, silt, clay, Chandina alluvium, valley alluvium, and so on; (iv) alluvial fan deposits: gravelly sand; (v) residual deposits; (vi) bedrock: Pleistocene and Pliocene; (vii) Tipam group: Pleistocene, Neogene, Tipam sand and stone; (viii) Surma group: Neogene, Miocene, and Oligocene; and (ix) major river.	Supervised classification [(Islam and Sado 2000a)]
Soil tract	(i) River and water body; (ii) hill tract: red clay soil, fine sand, and the mixture of two; (iii) Barind Tract: deep reddish brown terrace soils, gray, and silty and poorly drained; (iv) coastal saline tract: saline and alkaline; (v) Madhupur tract or red soil tract: well to moderately well-drained, reddish brown to yellow–brown, strongly to extremely acidic, friable clay soils over deeply weathered, red-mottled, and Madhupur clay; (vi) Gangetic alluvial: clay loam, sandy loam, calcareous and non acidic; (vii) Tista silt: weekly acidic; and (viii) Brahmaputra alluvial: loamy soil.	Supervised classification [(Islam et al. 2017; Shafapour Tehrani et al. 2017)]
Drainage area (%)	(i) 0 to 25; (ii) 25 to 50; (iii) 50 to 75; and (iv) Above 75.	Manual
Flood depth (m)	(i) 0 to 0.50 m; (ii) 0.51 to 1.00 m; (iii) 1.01 to 1.50 m; (iv) 1.51 to 2.00 m; and (v) 2.01 to 2.50 m.	Manual [(Tingsanchali and Karim 2005)]
Flood duration	(i) Very long; (ii) Long; (iii) Medium; (iv) Short; and (v) No flooding.	Manual [(Islam and Sado 2000a)]

## 2.5 Modeling Approaches

### 2.5.1 Artificial Neural Network (ANN)

ANN is a mathematical model of human perception that can be trained for performing a particular task on the basis of available dataset, especially to explore the relationship between inputs and outputs (Rauter and Winkler 2018; Valencia and Graña 2018). The most common type of ANN consists of three interconnected layers: (i) input layer, (ii) hidden layer, and (iii) output layer. The input layer receives data from different sources. The number of hidden layers and their neurons is often defined by trial and error (Elsafi 2014; Jain et al. 1996; Karsoliya 2012). The number of neurons in output layers is fixed by the application and is represented by the class being processed. In this study, one of the most commonly used neural network methods, i.e.; multilayer perceptron (MLP) neural network was adopted (Kia et al. 2012). To apply the MLP neural network, the back propagation (BP) algorithm with the sigmoid transfer functions was

used in the hidden and output layers. Then, all observations were presented to the network, the weights were determined from the model by considering nine input layers, five hidden layers, and one output layer to produce a flood susceptibility map. The neurons in the input layer denoted different conditioning factors. The numbers of the hidden layers were confirmed by running the MLP neural networks several times to gain compatible training and testing accuracies (Arora et al. 2004). The ANN model was trained with a maximum of 500 iterations and 10 tours with fivefold cross-validation. The convergence criterion was 0.00001. The probability of flood susceptibility (output layer) falls in the range between 0 and 1. When the percentage of the incorrect predictions in the neural network analysis decreased then the weights ( $w_i$ ) were stored to calculate flood susceptibility scores (FS). The Gradient Descent was used to estimate weights, where the initial learning rate, lower level learning rate, and the momentum were 0.4, 0.001, and 0.9, respectively. Moreover, the interval centre and interval offset were 0 and  $\pm 0.5$ , respectively. Basically, the weights were calculated by normalizing and

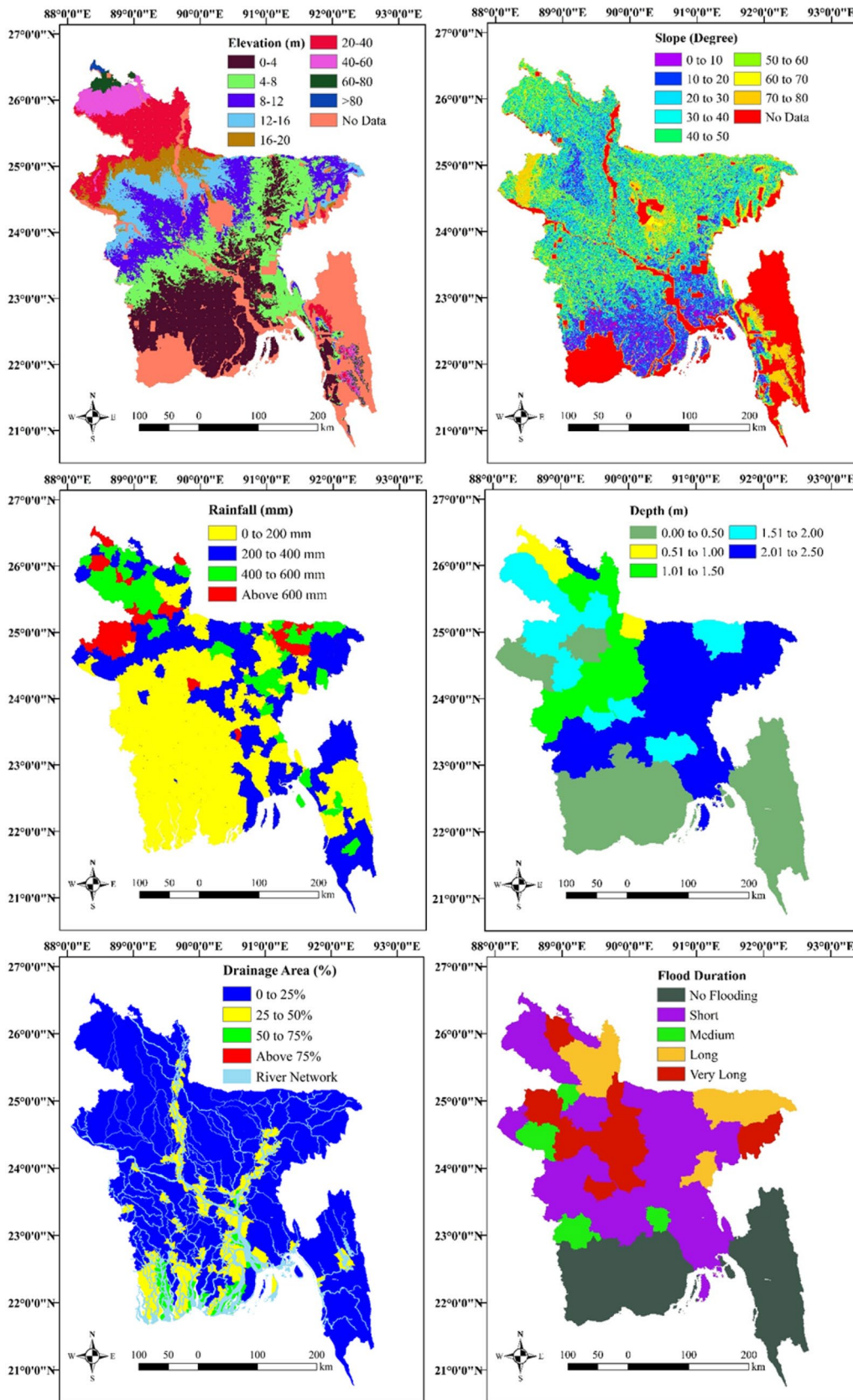


Fig. 2 Thematic maps used in this work

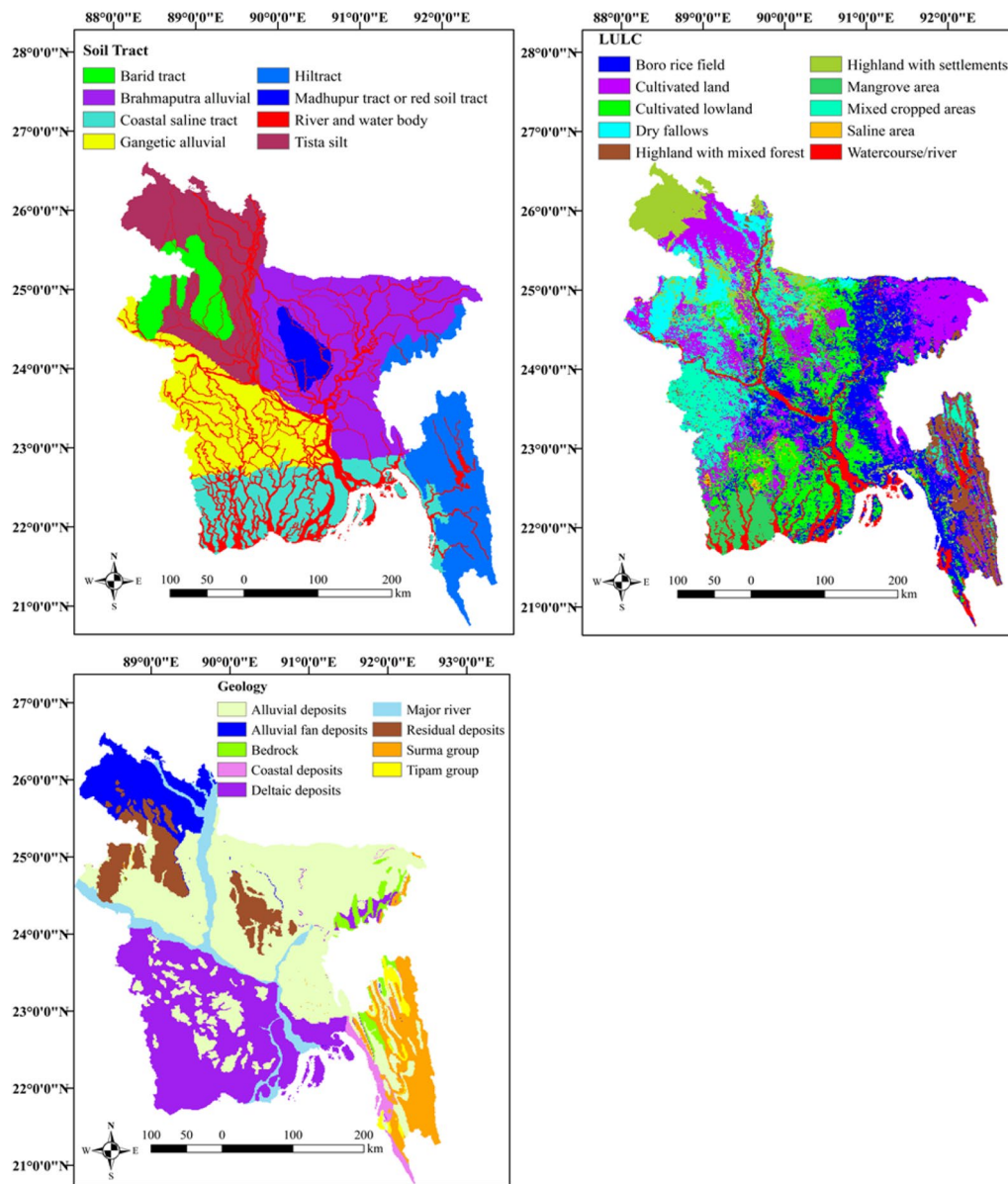


Fig. 2 (continued)

**Table 2** Multicollinearity test using tolerance (TOL) and variance inflation factor (VIF)

Conditioning factors	Collinearity		Conditioning factors	Collinearity	
	TOL	VIF		TOL	VIF
Rainfall	0.769	1.301	Soil tract	0.388	2.574
Elevation	0.486	2.057	Drainage area	0.902	1.108
Slope	0.772	1.296	Flood depth	0.460	2.172
LULC	0.545	1.834	Flood duration	0.500	2.000
Geology	0.412	2.428			

considering the variation of the maximum and minimum connection weights. The normalized values fall between 0 and 1. The mathematical expression for determining flood susceptibility scores is given as: (Kia et al. 2012).

$$FS = \sum_{i=1}^n w_i x_i = w_1 x_1 + w_2 x_2 + \dots + w_n x_n = w^T x, \quad (1)$$

where  $n$  is the number of flood conditioning factors,  $w_i$  is the weight coefficient of the flood conditioning factor

determined by ANN,  $x_i$  is the input value from each class of each conditioning factor. Here,  $T$  is the transpose of a matrix, and, in its simplest case, the output value FS is computed as:

$$FS = \begin{cases} 1 & \text{if } w^T x \geq \theta \\ 0 & \text{if otherwise} \end{cases}, \tag{2}$$

where  $\theta$  is the threshold level and this type of node is called as a linear threshold unit.

### 2.5.2 Analytical Hierarchy Process (AHP)

The AHP was used to determine the weighting factors ( $w_i$ ), which indicates the importance of each factor to the occurrence of floods. AHP refers to a structured tool to analyze difficult decisions, based on mathematics and psychology (Cho et al. 2015; Nguyen et al. 2015; Saaty 2000; Zhang et al. 2016). The pairwise comparison method was used to produce weighting factors by applying Saaty’s ranking scale (Luu et al. 2018; Saaty 2008) for each indicator, which was calculated and examined by the random consistency index (RI) (Luu et al. 2018; Saaty 2001). Saaty (1980) developed an average random consistency index (RI) for different matrix orders and defined the consistency ratio (CR), which is shown in Eq. (3), where the ratio of the consistency index (CI) is shown in Eq. (4) and the random consistency index (RI) (Luu et al. 2018; Rahmati et al. 2016c; Saaty 1980, 2008). If CR is greater than 0.1, the comparison matrix is inconsistent and should be revised. The score for each indicator was considered based on the experts’ opinion from the relevant field (academics, hydrologist, engineer), the literature review, and authors’ judgments. Furthermore, ranks for the calculation of normalized rank ( $Nr$ ) were assigned to each class of flood conditioning factors on the basis of the degree of damage, their influence, and contribution to flood hazard susceptibility. The higher the rank, the higher the influence is. The base point 0 is considered for the class with no probability of damages or influences and the increment of 1 indicates increased influence on flood (NOAA 2007). The  $Nr$  was calculated on the basis of the sum of the ranks assigned to each conditioning factor (Rahmati et al. 2016c). Finally, flood susceptibility map was produced using: (Rahmati et al. 2016c).

$$CR = \frac{CI}{RI}, \tag{3}$$

where CI represents the consistency index and RI is the average random consistency index of the judgment matrix.

$$CI = \frac{\lambda_{max} - n}{n}, \tag{4}$$

where  $\lambda_{max}$  is the largest eigenvalue derived from the paired comparison matrix,  $n$  is the number of the conditioning factor.

$$FS = \sum_{i=1}^n w_i \times Nr_i, \tag{5}$$

where  $n$  is number of the conditioning factor,  $w_i$  is the weighting factor, and  $Nr_i$  is the normalized rank.

### 2.5.3 Logistic Regression (LR)

LR is a multivariate statistical model for flood susceptibility mapping (Shafapour Tehrany et al. 2017; Tehrany et al. 2014a). The benefit of this model is that data do not require to be normally distributed and the factors can either be categorical, continuous, or any combination of both (Tehrany et al. 2019). In this model, flood susceptibility map developed from flood inundation area was considered as the dependent variable, where 1 is for flooding area and 0 is for non-flooding area. The mathematical expression of the LR model is given by: (Arabameri et al. 2018; Shafapour Tehrany et al. 2017; Tehrany et al. 2014a):

$$P = \frac{1}{1 + e^{-z}} = \frac{1}{[1 + e^{\{-(b_0 + b_1x_1 + b_2x_2 + b_3x_3 + \dots + b_nx_n)\}}]}, \tag{6}$$

where  $P$  is the probability of occurrence of flood or non-flood,  $z$  is the linear combination,  $n$  is the number of flood conditioning factors,  $x_i$  ( $i = 1, 2, 3 \dots n$ ) is the flood conditioning factors,  $b_0$  is the intercept of the model,  $b_i$  ( $i = 0, 1, 2, \dots, n$ ) is the regression coefficients for the independent variables of the logistic regression model.

### 2.5.4 Frequency Ratio (FR)

FR model is based on the observed relationships between the distribution of the floods and flood conditioning factor (Samanta et al. 2018b; Tehrany et al. 2019). The frequency ratio for the class of each conditioning factor was calculated by dividing the flood occurrence ratio by the area ratio. Each factor frequency ratio was calculated using Eq. (7) and flood susceptibility map was developed from Eq. (8) (Samanta et al. 2018b; Tehrany et al. 2019).

$$FR = \frac{\text{Percentage of flood}}{\text{Percentage of the class of each conditioning factor}}, \tag{7}$$

$$FS = FR_1 + FR_2 + FR_3 + \dots + FR_n, \tag{8}$$

where FR is the ranking of each conditioning factors,  $n$  is the number of total factors for flood susceptibility (FS).

### 2.5.5 Integrated Model

There were few weak points observed in individual models, as they do not generally yield desired result, therefore many researchers proposed integrated models to overcome weaknesses. For instance, this study proposed integrated models to develop flood susceptibility mapping in Bangladesh through the integration of two or more models to overcome the weakness and improve the prediction capability of the individual model. The following mathematical expression was considered to determine the best possible combination of the integrated models in assessing flood hazard. Then, the results from the individual models were considered to develop an integrated model using the following: (Arabameri et al. 2017; Pourghasemi et al. 2017).

$$nC_r = \frac{n!}{r!(n-r)!} = \frac{n(n-1)(n-2) \dots (n-r+1)}{r!}, \tag{9}$$

where  $n$  is number of the model and  $r$  is number of a set of the  $n$  model

$$IM_{nC_r} = \frac{\sum_{i=1}^n (AUROC_i \times M_i)}{\sum_{i=1}^n AUROC_i}, \tag{10}$$

where IM is the integrated model,  $AUROC_i$  is the AUROC value from the validation test of the single model, and  $M_i$  is the result of the single model (Fig. 3).

## 3 Results and Discussion

### 3.1 Application of the ANN Model

Determining the importance of flood conditioning factors using the ANN model showed that amongst nine factors, soil tract (19.30%), geology (17.20%), LULC (12.70%), elevation (11.40%), and flood depth (10.10%) had the highest impact on the occurrence of flood (Table 3). In contrast, flood duration (9.70%), drainage area (8.10%), slope (7.20%), and rainfall (4.30%) had the least contribution. Kia et al. (2012) noted that soil groups are the most important conditioning factors in flood susceptibility mapping using the ANN model; this is in accordance to this study. In other studies, slope, elevation, and LULC were the most important factors observed by ANN model in flood susceptibility mapping, which is consistent with the results our work (Chapi

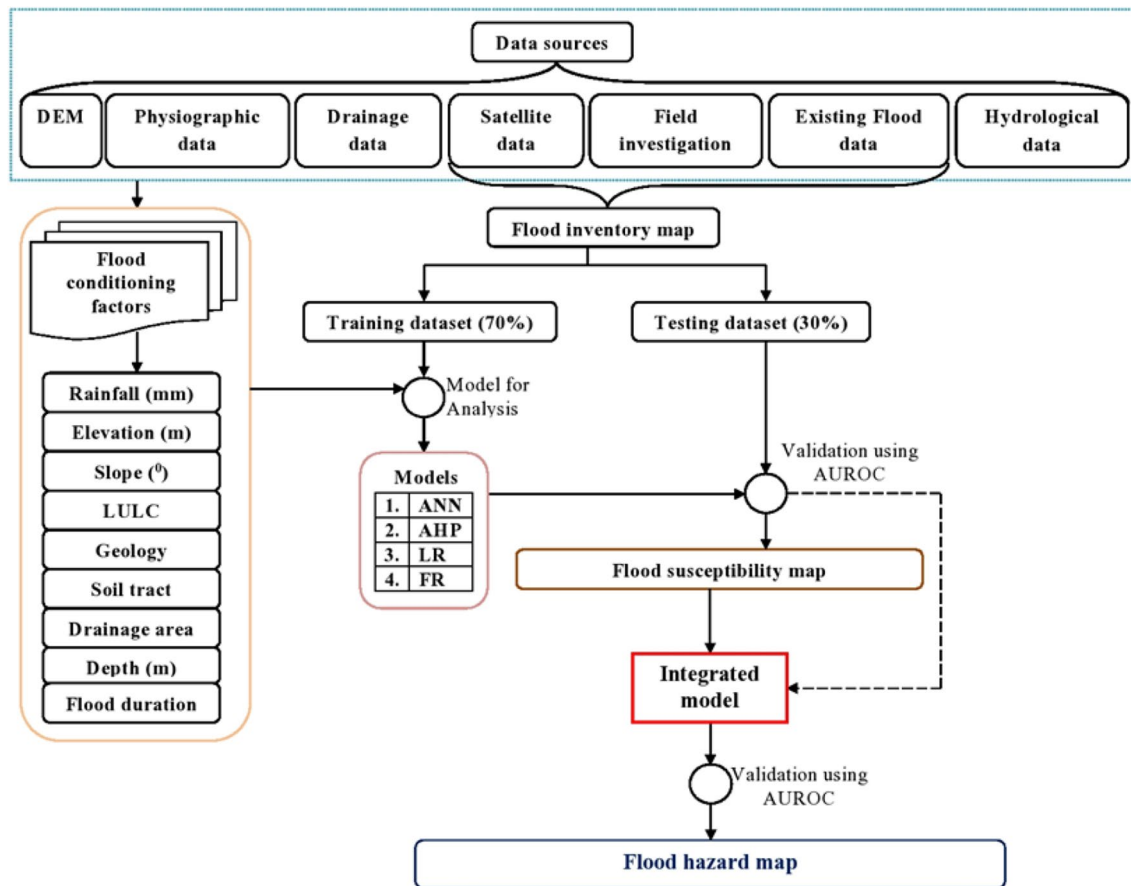


Fig. 3 Schematic diagram, showing overall methodology of the work

**Table 3** Flood conditioning factors used in susceptibility mapping

Flood conditioning factors	FR	Normal-ized rank ( $Nr_i$ )	AHP weight ( $w_i$ )	ANN weight ( $w_i$ )	LR coefficients ( $b_i$ )
Rainfall (mm)	1.04	0.40	0.22	0.043	0.225
	0.90	0.30			
	0.94	0.20			
	1.05	0.10			
Elevation (m)	1.06	0.20	0.142	0.114	- 0.227
	1.23	0.18			
	1.22	0.16			
	1.00	0.13			
	1.10	0.11			
	0.47	0.09			
	0.25	0.07			
	0.37	0.04			
	0.64	0.02			
Slope (°)	1.69	0.22	0.145	0.072	- 0.086
	1.23	0.19			
	0.99	0.17			
	0.91	0.14			
	0.89	0.11			
	0.90	0.08			
	0.89	0.06			
	0.93	0.03			
	0.93	0.03			
LULC	1.04	0.15	0.081	0.127	0.006
	1.27	0.16			
	1.35	0.18			
	0.69	0.11			
	0.94	0.13			
	0.50	0.02			
	0.30	0.04			
	0.78	0.05			
	1.77	0.07			
	0.64	0.09			
Geology	0.79	0.13	0.080	0.172	0.348
	0.81	0.16			
	1.50	0.20			
	0.44	0.09			
	0.65	0.11			
	0.40	0.07			
	0.35	0.04			
	0.06	0.02			
	1.08	0.18			
Soil tract	0.28	0.06	0.040	0.193	0.272
	0.16	0.03			
	0.59	0.08			
	1.07	0.11			
	1.48	0.19			
	1.17	0.17			
	1.08	0.14			
	1.79	0.22			

**Table 3** (continued)

Flood conditioning factors	FR	Normal- ized rank ( $Nr_i$ )	AHP weight ( $w_i$ )	ANN weight ( $w_i$ )	LR coefficients ( $b_i$ )
Drainage area (%)	1.13	0.40	0.130	0.081	-0.574
	0.67	0.30			
	0.09	0.20			
	0.00	0.10			
Flood depth (m)	1.27	0.27	0.082	0.101	0.042
	1.10	0.20			
	1.31	0.33			
	0.83	0.13			
	0.63	0.07			
Flood duration	1.16	0.20	0.080	0.097	0.656
	0.84	0.10			
	1.32	0.30			
	1.35	0.40			
	0.55	0.00			

et al. 2017; Falah et al. 2019; Mosavi et al. 2018). Finally, the resultant by ANN model was classified into four classes (low to very high) using the equal interval method (Fig. 4) (Samanta et al. 2018b; Tehrany et al. 2019). The output showed that 18.31% of study area belong to very high class, whereas 7.68% belong to low flood susceptibility (Table 3).

### 3.2 Application of the AHP Model

The degree of influence of rainfall to flood susceptibility is the highest, as evidenced by the weight of 0.220 through AHP method, while the slope factor was 0.145. The results of the optimized factor weights for flood conditioning factors are listed in Table 3. The elevation factor was considered less influencing compared with rainfall and slope (weight of 0.142). The weight factor for drainage area (%) was 0.130 also proved its importance in flood susceptibility analysis. The weight for both geology and flood duration was equal with 0.080. Flood depth, Land use/land cover, and soil tract were considered the least important as weights are 0.082, 0.081, and 0.040, respectively. Furthermore, normalized ranks for each condition factor were also calculated (Table 3). Then, the scores for flood susceptibility were estimated using Eq. (5) and prepared in the form of GIS data. Finally, the scores were classified into four categories as low (4.33%), medium (36.94%), high (51.98%), and very high (6.75%) (Fig. 4).

### 3.3 Application of the LR Model

The results of LR model showed that elevation, geology, soil tract, and flood duration factors were the most effective variables on flood susceptibility mapping, because

the significant (Sig,  $p$ ) values were less than 0.05. The rest of the conditioning factors have the Sig ( $p$ ) value of more than 0.05, suggesting statistically insignificant in the model development (Shafapour Tehrany et al. 2017, 2019; Tehrany et al. 2014a). Moreover, the positive and negative values of the output indicate their contribution to the occurrence of floods. Based on the derived logistic coefficients, probability of flood occurrence was calculated using Eq. (6) to develop flood susceptibility map, where the  $z$  values were calculated using the following:

$$\begin{aligned}
 z = & -2.230 + (0.225 \times \text{rainfall}) + (-0.227 \times \text{elevation}) \\
 & + (-0.086 \times \text{slope}) + (0.006 \times \text{LULC}) \\
 & + (0.348 \times \text{geology}) + (0.272 \times \text{soil}) \\
 & + (-0.574 \times \text{drainage}) + (0.042 \times \text{flood depth}) \\
 & + (0.656 \times \text{flood duration}). \quad (11)
 \end{aligned}$$

In Eq. (11), the probability values varied from 0 to 0.97. A flood susceptibility map was derived from LR model, which was then divided into four categories: low (22.38%), medium (24.90%), high (29.09%), and very high (23.62%) (Fig. 4).

### 3.4 Application of the FR Model

The results of FR model indicated that soil tract, rainfall, slope, elevation, and LULC are the most significant factors. This finding is in line with previous studies (Khosravi et al. 2016a; Samanta et al. 2018b; Shafapour Tehrany et al. 2017; Tehrany et al. 2019). The range of FR values varies from 0 to 1.79. The higher the value the higher the susceptibility to flood is. The results of the FR model are shown in

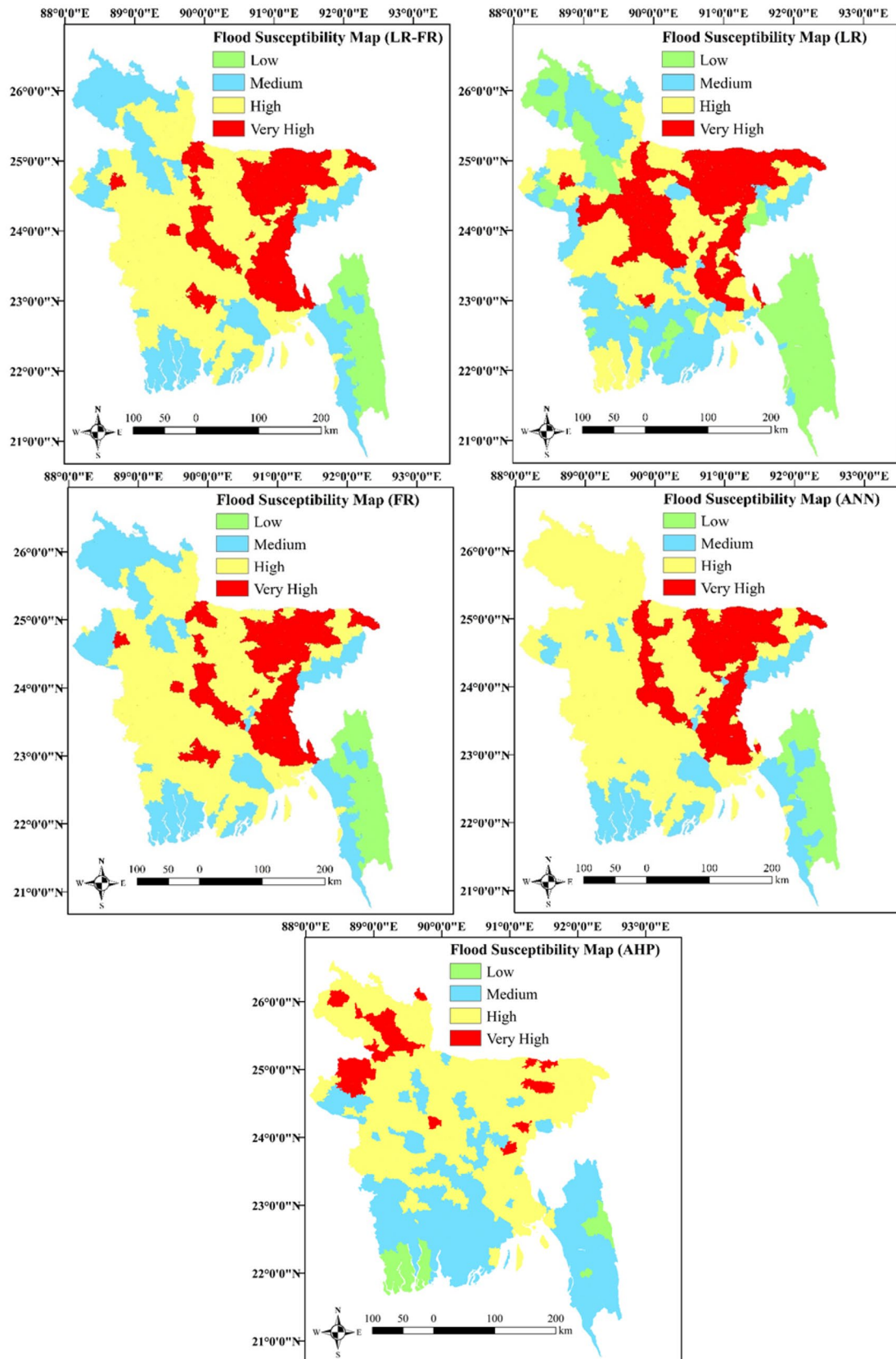


**Fig. 4** Flood susceptibility maps for Bangladesh with different models

Table 3, which confirmed that rainfall above 600 mm has a substantial impact on the occurrence of flood (with an FR value of 1.05). The relationship between elevation and flood susceptibility showed that low elevation category is more susceptible to flood, which is not surprising given that water tends to flow from highland to lowland. On the other hand, lower slope areas showed a greater correlation with flood occurrence compared with the higher slope. LULC factor supports that saline area (FR = 1.77) and cultivated lowland (FR = 1.35) have the greatest impact. Alluvial deposits class (FR = 1.50) of geological unit has a strong correlation with flood occurrence. The Brahmaputra alluvial soil tract has the highest FR value of 1.79. Therefore, susceptibility to flood occurrence is high in this class. The FR in drainage area indicates that flood occurrence decreased with the upper boundary of drainage area. The value of the highest FR = 1.13 lies in the drainage area of 0 to 25%. As far as the flood depth is concerned, depth of 1.01 to 1.50 m has the maximum FR (1.31). The results confirmed that this class plays a vital role in the occurrence of flood hazard in Bangladesh. In case of flood duration, long and very long duration with FR = 1.32 and FR = 1.35, are highly susceptible to flood. After determining FR of all classes, flood susceptibility map was developed using Eq. (7), whose values vary between 4.92 and 12.13. Finally, derived product was categorized into four classes from low to very high (Fig. 4).

### 3.5 Application of the Integrated Model

In this work, a total of eleven combinations of integrated models (e.g.  ${}_4C_2$ ,  ${}_4C_3$ , and  ${}_4C_4$ ) were produced using Eqs. (9), (10) to develop a reasonable flood hazard map.

In general, maps developed from the integrated models represented the better prediction accuracy than standalone models and can be used for the spatial prediction of flood hazard analysis in the study area. The outputs of the models were classified as low, medium, high, and very high susceptible, which showed that most of the flood-affected areas are located in high and very high categories. The combination which shows the maximum total of flood areas under high and very high susceptibility classes is considered as the best integrated model. The susceptibility map developed from  ${}_{11}C$  combination (LR-FR) indicated that 66.38% of the study area ranked high to very high, which is almost 91.49% of total flooding areas (Table 4). But, the  ${}_{09}C$  combination (AHP-LR) and  ${}_{10}C$  combination (AHP-FR) had the lowest result (Table 4). Therefore, flood susceptibility map developed from the  ${}_{11}C$  combination was considered as a new flood hazard map for Bangladesh, as it is predicted highest among all single and integrated models. Studies elsewhere also identified that integrated models are useful for hazard assessment (Choubin et al. 2019; Gazendam et al. 2016; Hong et al. 2018; Khosravi et al. 2016a; Mojaddadi et al. 2017; Shafapour Tehrani et al. 2019; Tehrani et al. 2015a). We, therefore, believe that the integrated models could be used for hazard analysis in other areas of similar environment.

Furthermore, the proposed maps developed from the models would be helpful for relevant authorities to take flood countermeasures that are valuable in reducing damages to economy. The results of this study can serve as the basis for prioritizing efforts, emergency response measures, channelizing funds, saving lives and properties, and policy interventions at the sub-district level. As for the

**Table 4** The best combination of thematic maps developed from ANN, AHP, LR, and FR models for flood hazard assessment in Bangladesh

Combination	Model				Area (%)				Flood area (%) under high and very high susceptibility classes
	ANN	AHP	LR	FR	Low	Medium	High	Very high	
–	■				7.68	17.38	56.63	18.31	89.18
–		■			4.33	36.94	51.98	6.75	70.97
–			■		22.38	24.90	29.09	23.62	89.27
–				■	8.41	26.10	46.95	18.54	86.62
${}_{01}C$	■	■	■	■	9.12	24.89	47.39	18.60	87.20
${}_{02}C$	■	■	■		12.89	21.23	48.17	17.71	86.64
${}_{03}C$	■	■		■	13.27	21.59	48.15	16.99	87.84
${}_{04}C$	■		■	■	9.12	24.89	47.39	18.60	87.20
${}_{05}C$		■	■	■	8.41	25.90	46.74	18.94	87.11
${}_{06}C$	■	■			10.12	23.64	44.64	21.60	90.50
${}_{07}C$	■		■		12.89	21.23	48.17	17.71	86.64
${}_{08}C$	■			■	11.14	22.67	48.97	17.22	87.98
${}_{09}C$		■	■		11.50	33.86	35.77	18.87	73.00
${}_{10}C$		■		■	11.71	33.78	35.69	18.82	72.94
${}_{11}C$			■	■	8.22	25.41	45.54	20.84	91.49

local society, communities should recognize and conform to early warnings, follow evacuation plans, and stay away from areas with high flood susceptibility.

### 3.6 Importance of Conditioning Factors In Mapping Flood Susceptibility

Determining the importance of conditioning factors in flood susceptibility mapping is essential in flood hazard assessment. However, different influencing factors contribute differently to flood hazard. Moreover, not all factors would have an equal effect on floods; thus, the selection of appropriate flood is a crucial step. The results showed that the most important conditioning factors according to the lambda and uncertainty coefficients were geology, soil tract, elevation, flood duration, LULC, and flood depth, because a value close to or equal to 1 means that the flood conditioning factors perfectly predict flood-susceptible areas, while a value of 0 shows that they do not have influence on floods (Table 5). In other works, researchers concluded that rainfall, soil, and geology have high importance (Ouma and Tateishi 2014; Seejata et al. 2018), consistent with our results. In another research, elevation and LULC were found to be the most influencing factors (Kourgialas and Karatzas 2011). Rahmati et al. (2016a) reported that slope has importance in the occurrence of floods, which is also in line with this study.

### 3.7 Models Validation and Performance for the Flood Susceptibility Maps

Derived flood susceptibility maps were validated with the AUROC. The AUROC of ANN, AHP, LR, and FR models for the validating datasets are shown in Fig. 5a. They showed that the AUROC value for the LR was 86.80%, while in the FR, ANN, and AHP models, the AUROC values were 85.60%, 82.10%, and 64.00%, respectively. Similarly, to evaluate the performance of these models training datasets were used to plot the AUROC. The results showed that AUROC values for flood susceptibility maps generated by LR, FR, ANN, and AHP models were 81.60%, 74.20%, 73.40%, and 70.60% (Fig. 5b). In other studies, FR model was compared with WoE and found that the FR model (AUROC = 76.47%) had higher prediction accuracy

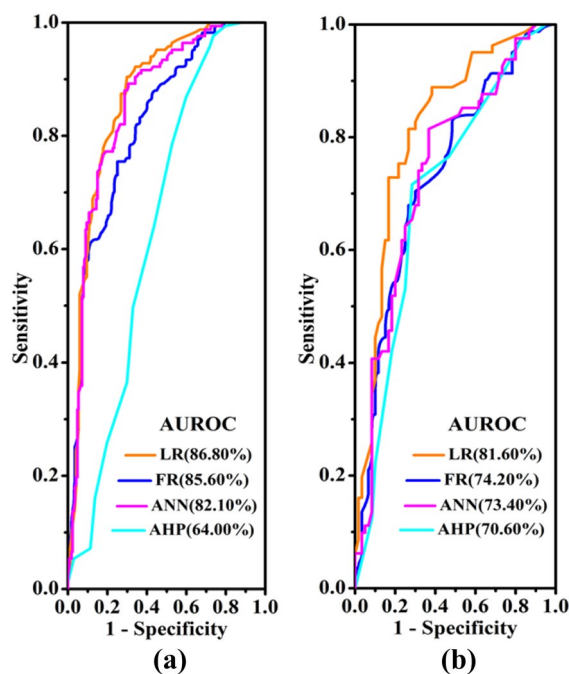
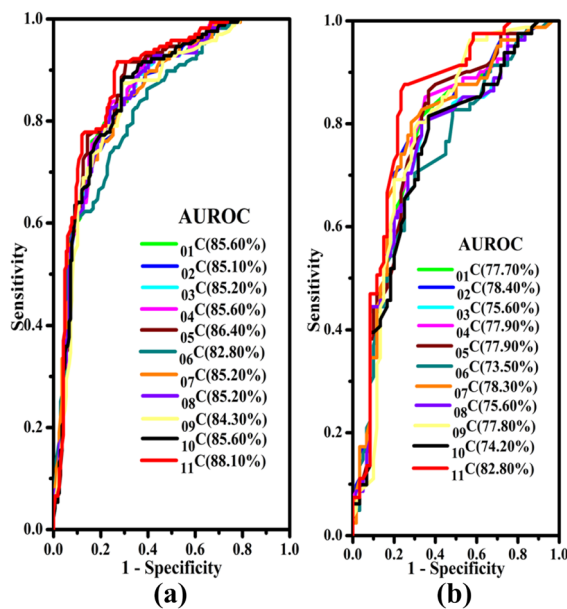


Fig. 5 The area under the receiver operating curves (AUROC) showing a validation and b performance of the proposed models

than WoE (AUROC = 74.74%), which is in accordance with current study (Rahmati et al. 2016b). Likewise, the AUROC success and prediction rate was estimated to be 84.80% and 81.20% in flood susceptibility mapping in India using frequency ratio technique (Samanta et al. 2018a). Bui et al. (2018) applied logistic regression (LR) model for flood prediction mapping in the Haraz watershed in northern province of Mazandaran, Iran, and stated that LR with AUROC = 88.5% was suitable for flood susceptibility as a standalone model. Our results are in line with Bui et al. (2018), as individual LR model had high accuracy and was suitable for delineating flood susceptibility. Therefore, the results of this study showed that the flood susceptibility map prepared by the LR model had higher predictive capacity compare with other three models. It is, therefore, reasonable to conclude that the LR model is the best choice, among the four individual models which can be useful for mapping hazard potential of similar settings.

**Table 5** Importance of conditioning factors in mapping flood susceptibility

Flood conditioning factors	Lambda	Uncertainty coefficient	Flood conditioning factors	Lambda	Uncertainty coefficient
Rainfall	0.090	0.008	Soil tract	0.503	0.300
Elevation	0.389	0.166	Drainage area	0.042	0.008
Slope	0.246	0.067	Flood depth	0.341	0.125
LULC	0.323	0.165	Flood duration	0.365	0.155
Geology	0.511	0.302			



**Fig. 6** The AUROC of the integrated models **a** validation and **b** performance of the proposed models

### 3.8 Validating Integrated Models

The results of integrated models showed that the AUROC was varying from 82.80 to 88.10% (Fig. 6a, b). In general, flood susceptibility maps developed from the integrated model (i.e.  $01C$ ,  $02C$ ,  $03C$ ,  $04C$ ,  $05C$ ,  $06C$ ,  $07C$ ,  $08C$ ,  $09C$ ,  $10C$  and  $11C$ ) presented better prediction accuracy than the individual models (i.e. ANN and AHP) for Bangladesh. The result of the integrated model ( $11C$ ) of LR and FR indicated that the accuracy for success (AUROC = 88.10%) is more from the individual model and the best among all integrated models; meanwhile, the accuracy of the ANN and AHP-integrated model ( $06C$ ), the AUROC = 82.80% was less than among all integrated models. In another research, it was stated that combination of adaptive neuro-fuzzy inference system (ANFIS) and imperialistic competitive algorithm (ICA) models with AUROC = 94.70% has high ability to identify susceptible areas to floods (Bui et al. 2018). Tehrany et al. (2019) used standalone frequency ratio, logistic regression, the WoE, and their ensemble techniques for spatially predicting flood-prone areas in Jiangxi Province, China. Their study indicated that integration of LR and FR models increased accuracy of AUROC (81.47%). The ANN-SVM integrated model showed highest predictive ability with AUROC of 87.90% for gully erosion mapping in Golestan Province, Iran. This underscores the efficacy of integrated models (Pourghasemi et al. 2017).

## 4 Conclusions

The conventional (hydraulic and hydrological) methods for flood susceptibility assessment require many parameters, which are usually lacking in Bangladesh. To overcome such a problem, we therefore, developed a method by integrating AHP, ANN, LR, and FR models. A total of eleven combinations of flood models (e.g.  $01C$  to  $11C$ ) were implemented for comparison purpose to determine the best model. Based on the results, following conclusions can be made:

(i) The prediction rate of the LR model (AUROC is 86.80%) is better than other models. Besides, the success rate showed that the LR model had the highest AUROC (81.60%), followed by the FR model (74.20%), ANN model (73.40%), and the AHP model (70.60%).

(ii) The accuracy of the integrated flood hazard map ( $11C$ ) was evaluated and it was found that 91.49% of the flooding areas were under high and very high susceptible categories, which rely on existing flood data. Besides, success and performance rate of integrated model was checked and the result showed that  $11C$  had the highest AUROC value of 88.10%, among other models tested here.

Overall, the models described in this study have the ability to elucidate better identification of flood hazard area. In addition, the results of this work have considerable management implications for disaster management of a highly populous country, which is at severe risk of climate-induced adversities such as flooding.

**Acknowledgements** The authors acknowledge and appreciate the provision of rainfall data by the Bangladesh Water Development Board (BWDB), without which this study would not have been possible. Thanks to AFM Kamal Chowdhury, Nirdesh Nepal and Soumik Nafis Sadeek for their valuable comments which helped us to improve the quality of the manuscript. This research was funded by the National Natural Science Foundation of China [Grant no. 41861134008 and 41671112] and the 135 Strategic Program of the Institute of Mountain Hazards and Environment (IMHE), Chinese Academy of Sciences (CAS) [Grant no. SDS-135-1705].

### Compliance with Ethical Standards

**Conflict of Interest** On behalf of all the authors, the corresponding author states that there is no conflict of interest.

## References

- Arabameri A, Pourghasemi HR, Yamani M (2017) Applying different scenarios for landslide spatial modeling using computational intelligence methods. *Environ Earth Sci* 76:832
- Arabameri A, Pradhan B, Rezaei K, Yamani M, Pourghasemi HR, Lombardo L (2018) Spatial modelling of gully erosion using evidential belief function, logistic regression, and a new ensemble of evidential belief function–logistic regression algorithm. *Land Degrad Dev* 29:4035–4049

- Arabameri A, Pradhan B, Rezaei K, Sohrabi M, Kalantari Z (2019) GIS-based landslide susceptibility mapping using numerical risk factor bivariate model and its ensemble with linear multivariate regression and boosted regression tree algorithms. *J Mt Sci* 16:595–618
- Arora M, Das Gupta A, Gupta R (2004) An artificial neural network approach for landslide hazard zonation in the Bhagirathi (Ganga) Valley, Himalayas. *Int J Remote Sens* 25:559–572
- Asare-Kyei D, Forkuor G, Venus V (2015) Modeling flood hazard zones at the sub-district level with the rational model integrated with GIS and remote sensing approaches. *Water* 7:3531–3564
- Ashley WS, Strader S, Rosencrants T, Krmeneć AJ (2014) Spatiotemporal changes in tornado hazard exposure: the case of the expanding bull's-eye effect in Chicago, Illinois. *Weather Clim Soc* 6:175–193
- Bangladesh Bureau of Statistics B (2019) Gender Statistics of Bangladesh, 2018. Bangladesh Bureau of Statistics (BBS) [http://bbs.portal.gov.bd/sites/default/files/files/bbs.portal.gov.bd/page/b343a8b4\\_956b\\_45ca\\_872f\\_4cf9b2f1a6e0/Gender%20Statistics%20of%20Bangladesh%202018.pdf](http://bbs.portal.gov.bd/sites/default/files/files/bbs.portal.gov.bd/page/b343a8b4_956b_45ca_872f_4cf9b2f1a6e0/Gender%20Statistics%20of%20Bangladesh%202018.pdf)
- Barua U, Akhter MS, Ansary MA (2016) District-wise multi-hazard zoning of Bangladesh. *Nat Hazards* 82:1895–1918
- Bates PD (2004) Remote sensing and flood inundation modelling. *Hydrol Process* 18:2593–2597
- Bui DT et al (2018) Novel hybrid evolutionary algorithms for spatial prediction of floods. *Sci Rep* 8:15364
- Bui DT, Ngo PTT, Pham TD, Jaafari A, Minh NQ, Hoa PV, Samui P (2019) A novel hybrid approach based on a swarm intelligence optimized extreme learning machine for flash flood susceptibility mapping. *Catena* 179:184–196
- Chapi K, Singh VP, Shirzadi A, Shahabi H, Bui DT, Pham BT, Khosravi K (2017) A novel hybrid artificial intelligence approach for flood susceptibility assessment. *Environ Modell Softw* 95:229–245
- Chen W, Pourghasemi HR, Naghibi SA (2018) A comparative study of landslide susceptibility maps produced using support vector machine with different kernel functions and entropy data mining models in China. *Bull Eng Geol Environ* 77:647
- Cho S, Kim J, Heo E (2015) Application of fuzzy analytic hierarchy process to select the optimal heating facility for Korean horticulture and stockbreeding sectors. *Renew Sustain Energy Rev* 49:1075–1083
- Choubin B, Moradi E, Golshan M, Adamowski J, Sajedi-Hosseini F, Mosavi A (2019) An Ensemble prediction of flood susceptibility using multivariate discriminant analysis, classification and regression trees, and support vector machines. *Sci Total Environ* 651:2087–2096
- Costache R, Zaharia L (2017) Flash-flood potential assessment and mapping by integrating the weights-of-evidence and frequency ratio statistical methods in GIS environment—case study: Bâsca Chiojdului River catchment (Romania). *J Earth Syst Sci* 126:59
- Danumah JH et al (2016) Flood risk assessment and mapping in Abidjan district using multi-criteria analysis (AHP) model and geoinformation techniques. *Geoenviron Disasters* 3:10
- Darabi H, Choubin B, Rahmati O, Haghghi AT, Pradhan B, Kløve B (2019) Urban flood risk mapping using the GARP and QUEST models: A comparative study of machine learning techniques. *J Hydrol* 569:142–154
- de Brito MM, Evers M (2016) Multi-criteria decision-making for flood risk management: a survey of the current state of the art. *Nat Hazards Earth Syst Sci* 16:1019–1033
- Department BF (2016) National Land Cover Classification System using LCCS v3. <http://bfis.bforest.gov.bd/library/wp-content/uploads/2018/12/108.pdf>. Accessed 30 Dec 2018
- Dewan AM, Islam MM, Kumamoto T, Nishigaki M (2007) Evaluating flood hazard for land-use planning in Greater Dhaka of Bangladesh using remote sensing and GIS techniques. *Water Resour Manag* 21:1601
- Elsafi SH (2014) Artificial neural networks (ANNs) for flood forecasting at Dongola Station in the River Nile, Sudan. *Alex Eng J* 53:655–662
- Falah F, Rahmati O, Rostami M, Ahmadisharaf E, Daliakopoulos IN, Pourghasemi HR (2019) Artificial neural networks for flood susceptibility mapping in data-scarce urban areas. In: Pourghasemi HR, Gokceoglu C (eds) *Spatial modeling in GIS and R for earth and environmental sciences*. Elsevier, pp 323–336
- Fenicia F, Kavetski D, Savenije HH, Clark MP, Schoups G, Pfister L, Freer J (2014) Catchment properties, function, and conceptual model representation: is there a correspondence? *Hydrol Process* 28:2451–2467
- Fernández D, Lutz M (2010) Urban flood hazard zoning in Tucumán Province, Argentina, using GIS and multicriteria decision analysis. *Eng Geol* 111:90–98
- Gazendam E, Gharabaghi B, Ackerman JD, Whiteley H (2016) Integrative neural networks models for stream assessment in restoration projects. *J Hydrol* 536:339–350
- Hasan S, Deng X, Li Z, Chen D (2017) Projections of future land use in Bangladesh under the background of baseline, ecological protection and economic development. *Sustainability* 9:505
- Hong H, Pradhan B, Xu C, Bui DT (2015) Spatial prediction of landslide hazard at the Yihuang area (China) using two-class kernel logistic regression, alternating decision tree and support vector machines. *Catena* 133:266–281
- Hong H, Tsangaratos P, Ilija I, Liu J, Zhu A-X, Chen W (2018) Application of fuzzy weight of evidence and data mining techniques in construction of flood susceptibility map of Poyang County, China. *Sci Total Environ* 625:575–588
- Hossain S (2015) Local level flood forecasting system using mathematical model incorporating WRF model predicted rainfall
- ICIMOD (2017) Bangladesh Flood Mapping 2017. <https://geoap.ps.icimod.org/BDFlood2017>. Accessed 01 Jan 2018 2017
- Islam M, Sado K (2000a) Flood hazard assessment in Bangladesh using NOAA AVHRR data with geographical information system. *Hydrol Process* 14:605–620
- Islam MM, Sado K (2000b) Development of flood hazard maps of Bangladesh using NOAA-AVHRR images with GIS. *Hydrol Sci J* 45:337–355
- Islam MM, Sado K (2002) Development priority map for flood countermeasures by remote sensing data with geographic information system. *J Hydrol Eng* 7:346–355
- Islam MA, Hasan MA, Farukh MA (2017) Application of GIS in general soil mapping of Bangladesh. *J Geogr Inf Syst* 9:604
- Jain AK, Mao J, Mohiuddin K (1996) Artificial neural networks: a tutorial. *Computer* 29:31–44
- Karsoliya S (2012) Approximating number of hidden layer neurons in multiple hidden layer BPNN architecture. *Int J Eng Trends Technol* 3:714–717
- Khosravi K, Nohani E, Maroufinia E, Pourghasemi HR (2016a) A GIS-based flood susceptibility assessment and its mapping in Iran: a comparison between frequency ratio and weights-of-evidence bivariate statistical models with multi-criteria decision-making technique. *Nat Hazards* 83:947–987
- Khosravi K, Pourghasemi HR, Chapi K, Bahri M (2016b) Flash flood susceptibility analysis and its mapping using different bivariate models in Iran: a comparison between Shannon's entropy, statistical index, and weighting factor models. *Environ Monit Assess* 188:656
- Khosravi K et al (2018) A comparative assessment of decision trees algorithms for flash flood susceptibility modeling at Haraz watershed, northern Iran. *Sci Total Environ* 627:744–755
- Kia MB, Pirasteh S, Pradhan B, Mahmud AR, Sulaiman WNA, Moradi A (2012) An artificial neural network model for flood simulation using GIS: Johor River Basin, Malaysia. *Environ Earth Sci* 67:251–264

- Kourgialas NN, Karatzas GP (2011) Flood management and a GIS modelling method to assess flood-hazard areas—a case study. *Hydrol Sci J* 56:212–225
- Lee MJ, Kang Je, Jeon S (2012) Application of frequency ratio model and validation for predictive flooded area susceptibility mapping using GIS. In: 2012 IEEE international geoscience and remote sensing symposium. IEEE, pp 895–898
- Lin L et al (2019) Improvement and Validation of NASA/MODIS NRT Global Flood Mapping Remote Sensing 11:205
- Luu C, Von Meding J, Kanjanabootra S (2018) Assessing flood hazard using flood marks and analytic hierarchy process approach: a case study for the 2013 flood event in Quang Nam, Vietnam. *Nat Hazards* 90:1031–1050
- Masood M, Takeuchi K (2012) Assessment of flood hazard, vulnerability and risk of mid-eastern Dhaka using DEM and 1D hydrodynamic model. *Nat hazards* 61:757–770
- Mojaddadi H, Pradhan B, Nampak H, Ahmad N, Ghazali AHb (2017) Ensemble machine-learning-based geospatial approach for flood risk assessment using multi-sensor remote-sensing data and GIS Geomatics. *Nat Hazards Risk* 8:1080–1102
- Mosavi A, Ozturk P, Chau K-w (2018) Flood prediction using machine learning models: literature review. *Water* 10:1536
- Nguyen AT, Nguyen LD, Le-Hoai L, Dang CN (2015) Quantifying the complexity of transportation projects using the fuzzy analytic hierarchy process. *Int J Project Manage* 33:1364–1376
- NOAA (2007) Risk and vulnerability assessment steps. Hazards analysis extended discussion. NOAA Coastal Services Center, Charleston, SC
- Nyarko BK (2002) Application of a rational model in GIS for flood risk assessment in Accra. *Ghana J Spat Hydrol* 2:1–14
- Ouma Y, Tateishi R (2014) Urban flood vulnerability and risk mapping using integrated multi-parametric AHP and GIS: methodological overview and case study assessment. *Water* 6:1515–1545
- Pham BT, Bui DT, Prakash I, Dholakia M (2017) Hybrid integration of Multilayer Perceptron Neural Networks and machine learning ensembles for landslide susceptibility assessment at Himalayan area (India) using GIS. *Catena* 149:52–63
- Pourghasemi HR, Yousefi S, Kornejady A, Cerdà A (2017) Performance assessment of individual and ensemble data-mining techniques for gully erosion modeling. *Sci Total Environ* 609:764–775
- Pradhan B, Lee S (2010) Landslide susceptibility assessment and factor effect analysis: backpropagation artificial neural networks and their comparison with frequency ratio and bivariate logistic regression modelling. *Environ Modell Softw* 25:747–759
- Rahman AA, Alam M, Alam SS, Uzzaman MR, Rashid M, Rabbani G (2007) Risks, vulnerability and adaptation in Bangladesh. *Hum Dev Rep* 8
- Rahmati O, Haghizadeh A, Pourghasemi HR, Noormohamadi F (2016a) Gully erosion susceptibility mapping: the role of GIS-based bivariate statistical models and their comparison. *Nat Hazards* 82:1231–1258
- Rahmati O, Pourghasemi HR, Zeinivand H (2016b) Flood susceptibility mapping using frequency ratio and weights-of-evidence models in the Golastan Province, Iran. *Geocarto Int* 31:42–70
- Rahmati O, Zeinivand H, Besharat M (2016c) Flood hazard zoning in Yasooj region, Iran, using GIS and multi-criteria decision analysis. *Geomat Nat Hazards Risk* 7:1000–1017
- Rao D (2017) Hydrological and hydrodynamic modeling for flood damage mitigation in Brahmaniâ Baitarani River Basin, India. *Geocarto Int* 32:1004–1016
- Rauter M, Winkler D (2018) Predicting Natural Hazards with Neuronal Networks arXiv preprint [arXiv:180207257](https://arxiv.org/abs/180207257)
- Rizeei HM, Pradhan B, Saharkhiz MA (2019) Allocation of emergency response centres in response to pluvial flooding-prone demand points using integrated multiple layer perceptron and maximum coverage location problem models. *Int J Disaster Risk Reduction*:101205
- Saaty TL (1980) *The Analytic (Hierarchy) Process*. St Louis ua, New York
- Saaty TL (2000) *Fundamentals of decision making and priority theory with the analytic hierarchy process*, vol 6. Rws Publications, Pittsburgh
- Saaty TL (2001) *The seven pillars of the analytic hierarchy process*. In: Köksalan M, Zionts S (eds) *Multiple criteria decision making in the new millennium*. Springer, Berlin, Heidelberg, pp 15–37
- Saaty TL (2008) *Decision making with the analytic hierarchy process*. *Int J serv Sci* 1:83–98
- Sahoo SN, Sreeja P (2015) Development of Flood Inundation Maps and quantification of flood risk in an Urban catchment of Brahmaputra River ASCE-ASME. *J Risk Uncertain Eng Syst* 3:A4015001
- Samanta RK, Bhunia GS, Shit PK, Pourghasemi HR (2018a) Flood susceptibility mapping using geospatial frequency ratio technique: a case study of Subarnarekha River Basin, India. *Model Earth Syst Environ* 4:395–408
- Samanta S, Pal DK, Palsamanta B (2018b) Flood susceptibility analysis through remote sensing, GIS and frequency ratio model. *Appl Water Sci* 8:66
- Seejata K, Yodying A, Wongthadam T, Mahavik N, Tantane S (2018) Assessment of flood hazard areas using Analytical Hierarchy Process over the Lower Yom Basin, Sukhothai. *Province Procedia Eng* 212:340–347
- Shafapour Tehrany M, Shabani F, Neamah Jebur M, Hong H, Chen W, Xie X (2017) GIS-based spatial prediction of flood prone areas using standalone frequency ratio, logistic regression, weight of evidence and their ensemble techniques. *Geomat Nat Hazards Risk* 8:1538–1561
- Shafapour Tehrany M, Kumar L, Neamah Jebur M, Shabani F (2019) Evaluating the application of the statistical index method in flood susceptibility mapping and its comparison with frequency ratio and logistic regression methods. *Geomat Nat Hazards Risk* 10:79–101
- Sinha DK (2007) *Natural disaster reduction: South East Asian realities, risk perception and global strategies*. Anthem Press, London
- Tehrany MS, Lee M-J, Pradhan B, Jebur MN, Lee S (2014a) Flood susceptibility mapping using integrated bivariate and multivariate statistical models. *Environ Earth Sci* 72:4001–4015
- Tehrany MS, Pradhan B, Jebur MN (2014b) Flood susceptibility mapping using a novel ensemble weights-of-evidence and support vector machine models in GIS. *J Hydrol* 512:332–343
- Tehrany MS, Pradhan B, Jebur MN (2015a) Flood susceptibility analysis and its verification using a novel ensemble support vector machine and frequency ratio method. *Stoch Environ Res Risk Assess* 29:1149–1165
- Tehrany MS, Pradhan B, Mansor S, Ahmad N (2015b) Flood susceptibility assessment using GIS-based support vector machine model with different kernel types. *CATENA* 125:91–101
- Tingsanchali T, Karim MF (2005) Flood hazard and risk analysis in the southwest region of Bangladesh. *Hydrol Process* 19:2055–2069
- Todini F, De Filippis T, De Chiara G, Maracchi G, Martina M, Todini E (2004) Using a GIS approach to assess flood hazard at national scale. In: *Proceedings of the European Geosciences Union, 1st General Assembly, Nice, 25–30 April 2004*
- Uddin K, Matin MA, Meyer FJ (2019) Operational flood mapping using multi-temporal sentinel-1 SAR images: a case study from Bangladesh. *Remote Sens* 11:1581
- Valencia JA, Graña AM (2018) A neural network model applied to landslide susceptibility analysis (Capitanejo, Colombia) *Geomatics. Nat Hazards Risk* 9:1106–1128
- Yang T-H, Ho J-Y, Hwang G-D, Lin G-F (2014) An indirect approach for discharge estimation: a combination among micro-genetic algorithm, hydraulic model, and in situ measurement. *Flow Meas Instrum* 39:46–53
- Zhang W, Lu J, Zhang Y (2016) Comprehensive evaluation index system of low carbon road transport based on fuzzy evaluation method. *Procedia Eng* 137:659–668